

# Exploring New Active Materials for Low-Noise Room-Temperature Microwave Amplifiers and Other Devices

Aharon Blank, Raphael Kastner, *Senior Member, IEEE*, and Haim Levanon

**Abstract**—Newly discovered chemical systems, mainly the  $C_{60}$  molecule (a molecule containing 60 carbon atoms) and porphyrin molecules (one of the basic building blocks of the hemoglobin and chlorophyll molecules) dissolved in organic solvents, have been considered as active microwave amplifying or absorbing materials. These effects are obtained under an external dc magnetic field as well as optical excitation. These materials are potentially important in certain applications in microwaves. In this paper, an attempt is made at evaluating this potential. To this end, the complex permeability of the dissolved  $C_{60}$  molecules has been measured, under the aforementioned physical conditions, in three different experiments with the aid of three types of electron paramagnetic resonance (EPR) spectrometers, respectively. The permeability of the  $C_{60}$  molecules, when dissolved in liquid toluene, has been found to have a negative imaginary part of about  $\mu_r'' = -0.0055$  (i.e., attenuating for the  $e^{j\omega t}$  harmonic time dependence) over a bandwidth of 0.4 MHz around the center frequency, which is known as the Larmor frequency, and is determined by the external dc magnetic field. Alternatively, the same molecules, when dissolved in a nematic liquid crystal (LC), have either positive (amplifying) or negative (absorbing)  $\mu_r''$ , with absolute value of about 0.005 over a bandwidth of 27 MHz. All measurements have been taken around the temperature of  $T = 253$  K. The lifetime of the phenomenon, during the time span that follows the laser optical excitation, is about 10  $\mu$ s. The applicability of those materials for solid state optically pumped maser amplifiers, which operate at room temperature with a very low-noise temperature or for other novel devices, is demonstrated in this paper.

**Index Terms**—Active microwave materials, electron spin resonance, low-noise amplifiers, masers.

## I. INTRODUCTION

### A. Background

SINCE their invention [1] and fabrication [2], solid-state cavity masers [3] and traveling-wave masers [4], [5], which are based on electron paramagnetic resonance (EPR), have been used in a variety of applications, especially those which exploit their low-noise figure as microwave sources and microwave amplifiers [6]–[8]. However, in the 1970's and 1980's, the interest in such devices declined, mainly due to the fact that they operate at very low cryogenic temperatures, typically equal to 1.5 K, a fact which poses

severe realization difficulties. In addition, devices such as field-effect transistors (FET's), high electron-mobility transistors (HEMT's) or parametric low-noise amplifiers, when cooled to these temperatures, can also achieve a very low-noise temperature [9], [10]. A fairly simple thermoelectric cooling technique is usually used to cool these devices to moderate temperatures in order to achieve noise temperatures of about 35–200 K in the microwave region (note that noise temperature normally rises with frequency). It should be noted, nonetheless, that maser amplifiers are still in use for such applications as deep-space communications and radio telescopes [11], where ultra-low-noise performance is required.

Conventional EPR-based solid-state masers must operate at cryogenic temperatures because the pumping frequency is in the microwave region. Operation at room temperature would lead to a low inversion ratio, which is characterized by an almost equal Boltzmann distribution of the different microwave energy levels (i.e.,  $h\nu \ll K_b T$ , where  $h$  is Planck's constant,  $\nu$  is the frequency,  $K_b$  is the Boltzmann's constant, and  $T$  is the temperature in kelvin). Another and more dominant reason for operating in the low-temperature regime is the fact that the Zeeman levels life time ( $T_1$ ) in the paramagnetic crystals used by these masers falls off rapidly as temperature rises, reaching just a few nanoseconds or less at room temperature [4]. This short lifetime would imply an unrealistically high pumping power, thereby excluding the possibility of maser operation in both the continuous wave (CW) mode and the pulsed mode; such a short lifetime does not allow the maser signal to build up properly, hence, amplification is not feasible.

A successful attempt to overcome the first obstacle mentioned above was made with an optically pumped solid-state maser that was first proposed in 1957 [12] and demonstrated successfully in 1962 [13]. These kinds of devices can theoretically retain high inversion ratio and low-noise temperature at temperatures as high as room temperature [14], [15]. However, practical devices are still limited by the short lifetime of the Zeeman levels and cannot operate above approximately 100 K.

Recently, extensive research has been reported in the chemical community regarding the optically excited EPR spectrum of a variety of chemical materials [16]–[18]. Some of these materials exhibit high selectivity in the population of the spin levels at the time interval that immediately follows the optical excitation. All such investigations have been performed using fairly complicated EPR spectrometers, which

Manuscript received December 22, 1997; revised August 12, 1998.

A. Blank and R. Kastner are with the Department of Electrical Engineering-Physical Electronics, Tel-Aviv University, Tel-Aviv 69978, Israel.

H. Levanon is with the Department of Physical Chemistry, Hebrew University, Jerusalem 91904, Israel.

Publisher Item Identifier S 0018-9480(98)09035-8.

render the magnetic susceptibility in *normalized units only*, as a function of magnetic field. However, for engineering purposes, one would require an actual evaluation of the magnetic susceptibility of the materials under investigation in order to assess the possible benefits of these materials. To date, such information is not available in the context of the aforementioned investigations.

### B. Objectives of This Paper

Our investigations have focused on the evaluation of the permeability of photo-excited  $C_{60}$  molecules dissolved in liquid toluene and liquid crystal (LC),<sup>1</sup> in terms of absolute rather than arbitrary units as a function of frequency in a given dc magnetic field. Finding these permeability values enabled us at this stage to further assess the applicability of these materials for use in a number of conventional as well as novel microwave devices. The methods used in this paper also enable the investigation of additional chemical systems, which are best suited for the applications listed below. Based on these results, a demonstration of one of these applications is now being investigated.

One very promising application of these materials is in their use as active amplifying substances in optically pumped solid-state maser amplifiers operating at room temperature. We use the term “solid-state,” although we are dealing with liquids at room temperature, in order to make a distinction between these and gas masers. The latter ones are very weak in terms of both self-oscillating microwave power and microwave-amplification saturation power as compared with solid or liquid phase masers. This application would exploit the positive imaginary permeability values of these materials for the amplification of electromagnetic (EM) radiation with very low-noise temperature. The low-noise temperature is achieved by virtue of the low negative temperature of the optically pumped spin system.<sup>2</sup> Details are given below.

Other applications would take advantage of the following properties of these materials: the optically excited spin levels are easily saturated by EM radiation of the order of magnitude of 1 mW to create an EM limiting device. Such a device protects sensitive receivers from strong incoming EM signals. Further uses may be found by exploiting the special time dependency of the permeability following laser excitation or other special EM features listed below. As stated above, this paper deals with methods which quantitatively evaluate the permeability of materials subject to light excitation and an external dc magnetic field, and can also assess the applicability of the properties measured as to their use in several conventional and novel EM devices.

Three types of EPR experiments detailed in Section II made the quantitative evaluation of the permeability possible. A fourth experiment, which shall demonstrate and assess the materials as active maser materials, is both undergoing and presented (in its theoretical aspects) in Section III.

<sup>1</sup>We have used the LC *E* - 7, which contains the following materials:  $R_i$ -Ph-CN, where Ph is phenol ring and  $R_1 = C_5H_{11}$  in 51%,  $R_2 = C_7H_{15}$  in 25%,  $R_3 = C_8H_{17}O$  in 16%,  $R_4 = C_5H_{11}Ph$  in 8%.

<sup>2</sup>For details of electron spin-system temperature definition, see [19].

## II. THE MAGNETIC PROPERTIES OF $C_{60}$ IN TOLUENE AND LC

Normally, the  $C_{60}$  molecule, due to its highly symmetrical structure, is not EPR active. However, after irradiation with UV or visible light, a transient EPR signal will appear. This signal is assigned to the photo-excited triplet state of  $C_{60}$  ( $^3C_{60}$ ) [17].

Previous research has shown the existence of a mechanism which leads to selective population by selective intersystem crossing in the triplet  $^3C_{60}$  molecule, thereby causing the EPR spectrum of  $C_{60}$  in LC to have a non-Boltzmannian distribution [16]. It has been shown that it is quite likely that the selective population results in a situation with underpopulated and overpopulated spin states [18], [20] which will generate positive or negative imaginary spin susceptibility (depending on the dc magnetic field at a given frequency). However, as mentioned above, these works revealed only the photophysical and photochemical side of the phenomenon, and did not include absolute values of the material susceptibility. In this paper, an attempt is made to quantitatively evaluate this transient phenomenon and exploit the well-known fact that EPR-based solid-state masers use an inverted population energy-level system (i.e., have positive imaginary magnetic susceptibility) [21], with the objective of estimating the potential of this phenomenon for engineering applications.

Measurement of the ac susceptibility of stable materials with  $|\chi''| \ll 1$  is feasible using a number of methods [22], [23] (where  $\chi''$  is the imaginary part of the magnetic susceptibility per material quantity). On the other hand, we are dealing here with a transient phenomenon which may potentially generate values of the order of  $|\chi''| \approx 1$ . Consequently, we have been forced to use three different EPR spectrometers in order to obtain quantitative results. These measurements are described in the remainder of this section.

The first measurement involved investigation of  $C_{60}$  in toluene and LC, and was performed using a time-resolved EPR spectrometer [24]. This device measures the susceptibility of very short processes either as a function of time for a given dc magnetic field and frequency or as a function of the dc magnetic field for a given frequency and time. In our experiments, this device has been used to measure the susceptibility of the  $C_{60}$  molecules, following the laser pulse excitation. Details of the experiment apparatus are given in [24]. The measured susceptibility of  $C_{60}$  in liquid toluene and LC as a function of the magnetic field on the same arbitrary scale at a frequency of 9.14 GHz is shown in Fig. 1. The results for both solvents are shown together, although they have been measured separately in [16] and [18], with the aid of signal-to-noise ratio (SNR) estimations and knowledge of the spin dynamics [20], [25]. This is done as follows: one can see that the signal level of  $C_{60}$  in toluene is somewhat above noise level at the time that shortly follows the laser's excitation (see [16], [18], and Fig. 1). The time dependency of this signal, reported in [25], shows that the signal evolves to its maximum at about 2.7  $\mu s$  after lasers excitation and that its amplitude at 0.3  $\mu s$  after excitation is about 0.25 of the maximum amplitude [25], thus providing us with a good estimate of the SNR levels in the previously reported experiments [16], [18] and helping

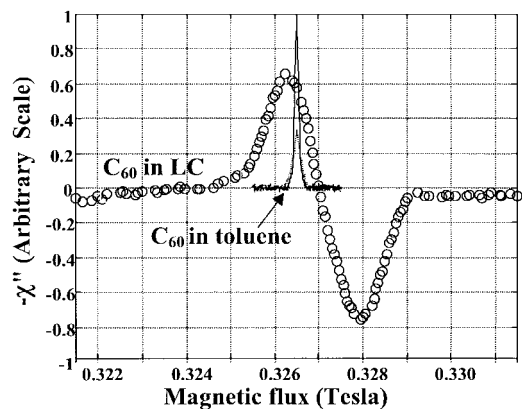


Fig. 1. The imaginary part of the magnetic susceptibility of  $C_{60}$  molecules in toluene at 253 K and in LC at 243 K. Solid line: the spectrum of  $C_{60}$  in toluene 2.7  $\mu$ s after laser pulse excitation. Dashed line: the spectrum of  $C_{60}$  in toluene 0.3  $\mu$ s after laser pulse excitation. Circles: the spectrum of  $C_{60}$  in LC 0.3  $\mu$ s after laser pulse excitation. Results were measured by time-resolved EPR spectrometer. The toluene spectrum lines were shifted by 5 G for convenience.

incorporate the measurements in [16] and [18] into Fig. 1. The error estimated from this combination is a factor of two.

One can also see in Fig. 1 that only a single absorption peak (i.e., negative imaginary susceptibility) exists in liquid toluene. This is due to the fast rotation of the molecules which tends to average the zero field splitting (ZFS) factor to zero. On the other hand, this averaging effect does not occur in LC in the nematic phase, and the spin energy levels of the triplet are selectively populated [16], [26]. Therefore, in this case, the sign of the imaginary part of the susceptibility is dependent upon the magnetic field. The time-resolved EPR spectrometer results cannot be calibrated because common materials with known ac susceptibility, which are used to calibrate ordinary EPR spectrometers results, also have time-independent susceptibility [22], which is subtracted in the time-resolved mechanism (the detector is ac-coupled to reduce noise).

In the second measurement, we used a Fourier-transform EPR spectrometer. This device monitors substances with a narrow EPR spectrum, both time constant and time dependent, and enables the possibility to jointly view the susceptibilities of  $C_{60}$  in liquid toluene and of solid 1,1-diphenyl-2-picrylhydrazyl (DPPH), the latter being used as a reference material with a quantitatively known measured signal, if its quantity is known. Our measurement consisted of  $C_{60}$  in liquid toluene in a concentration of  $10^{-3}$  mol/L at an irradiated sample volume of  $0.07 \text{ cm}^3$ , which we added on the sample tube (glued outside the sample) by yet unknown amount of solid DPPH grains. Both substances have a very narrow spectrum. The first one is transient, while the other one is stable. The susceptibility of these two materials as measured jointly, still in an arbitrary susceptibility scale, as a function of the magnetic field is presented in Fig. 2. The quantity of DPPH used in the Fourier-transform measurement was determined by performing the third measurement in a conventional CW EPR spectrometer with a special calibrating substance (“strong-pitch”),<sup>3</sup> which has a known number of effective spins in the

<sup>3</sup>Reference Manual for Instrumentation Bruker EPR Spectrometer Model 380E, Bruker Analytik GmbH, Germany, 1991

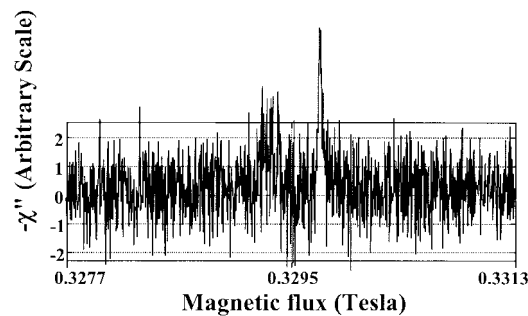


Fig. 2. The imaginary part of the magnetic susceptibility of  $C_{60}$  in liquid toluene, 2.7  $\mu$ s after laser pulse excitation together with grains of solid DPPH as a function of the magnetic field at a frequency of 9.295 GHz. Results obtained by Fourier-transform EPR at a temperature of 253 K.

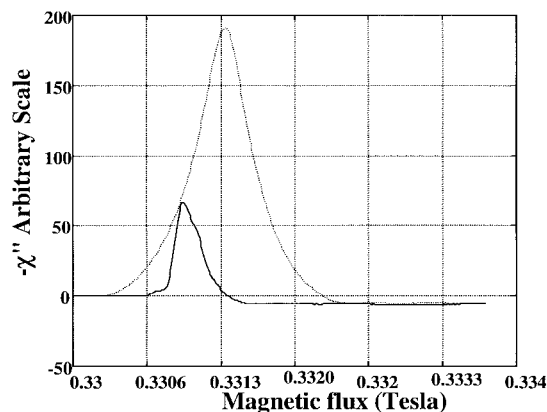


Fig. 3. The imaginary part of the magnetic susceptibility of solid DPPH grains (solid line) and “strong-pitch” (dashed line) as a function of the magnetic field as measured in “conventional” EPR spectrometer.

given sample size:  $7.5 \times 10^{15}$  (leading to known ac magnetic susceptibility). These two measurements are shown together in Fig. 3. By integrating the susceptibilities to obtain the area below the graphs of Fig. 3, one can estimate the number of spins contributing to the signal of DPPH as 1/8.5 of the “strong-pitch” signal or about  $9 \times 10^{14}$  spins. In Fig. 3, it can be deduced that the area below the DPPH signal is about  $3 \times$  larger than that of the signal of  $C_{60}$  in toluene, leading to the conclusion that about  $3 \times 10^{14}$  spins contributed to the  $C_{60}$  signal. This number is comparable to prior assessments of thermal equilibrium of the resultant signal [16], [25]. Fig. 1 shows (again, via integration of the curve) that the number of spins contributing to the signal of  $C_{60}$  in LC is about  $50 \times$  larger than those of  $C_{60}$  in toluene, leading to the fact that approximately  $1.5 \times 10^{16}$  spins contributed to the signal of  $C_{60}$  in LC. From this effective spin number and the sample volume, the ac susceptibility can be derived using the following relationships.

The power absorbed in a  $2J + 1$  energy-level system, as a result of an  $m_{J-1}$  to  $m_J$  magnetic transition is [27]

$$\begin{aligned} W(m_J) &= \Delta N (h\nu) p(m_J) \\ &= \Delta N (h\nu) (\pi/4) \gamma^2 H_1^2 (J + m_J)(J - m_J + 1) \\ &\quad \cdot f(w - w_0) \end{aligned} \quad (1)$$

where  $\Delta N$  is the spin population difference between the

levels  $m_{J-1}$  and  $m_J$ ,  $\nu$  is the microwave frequency,  $h$  is the Planck constant,  $\gamma = g\mu_B/\hbar$  is the electron-gyro magnetic ratio,  $H_1$  is the ac magnetic-field amplitude,  $f(\omega - \omega_0)$  is a normalized absorption/emission-line function, and  $p(m_J)$  is the probability of transition per time unit. It is known that the absorbed power in a magnetic material with imaginary volume magnetic susceptibility  $\kappa''$  (not to be confused with our measured results of  $\mathcal{X}''$  above) at frequency  $\omega$  is

$$W = \frac{1}{2} \omega \kappa'' H_1^2. \quad (2)$$

From (1) and (2), we have

$$\kappa'' = \frac{\Delta N}{4} h \gamma^2 (J + m_J) \cdot (J - m_J + 1) f(\omega - \omega_0). \quad (3)$$

In our case, we take  $J = 1$  (triplet state) and  $m_J = 0$ . The value of  $f(\omega - \omega_0)$  at resonance can be estimated by taking an acceptable Lorentzian line shape and looking at our measured linewidth results, thereby obtaining the ac susceptibility and arriving at the conclusion that the imaginary part of the ac volume magnetic permeability of  $C_{60}$  in LC, under dc magnetic field, at a concentration of  $10^{-3}$  mol/L,  $T = 253$  K and, following laser pulse excitation, is about  $\mu_r'' = 0.005$  over a bandwidth of 27 MHz. This is the absolute value of the imaginary permeability, which, as can be seen in Fig. 1, may be either positive (emission) or negative (absorption) depending on the frequency and dc applied magnetic field. Lifetime of the phenomenon is about 10  $\mu$ s [20]. For  $C_{60}$  in liquid toluene, similar values are observed, however, only in a bandwidth of about 0.4 MHz and for negative imaginary permeability values.

### III. $C_{60}$ IN LC AS A MASER MATERIAL

This section deals with both the fourth experiment and with the theory which is used to assess the capability of the above material as an active maser amplifier device. The following five aspects of the maser phenomenon are considered:

- 1) noise temperature;
- 2) gain-loss balance;
- 3) pumping power;
- 4) oscillation buildup time;
- 5) maximum gain, bandwidth, and saturation power.

We first briefly describe the numerical electromagnetic procedure developed to evaluate the scattering matrix parameters of a cylindrical sample inside a rectangular waveguide and the experimental process of validating the numerical model. A cylindrical sample was chosen because it is the natural way of employing liquid samples inside a waveguide, it is commonly used in EPR experiments and, in fact, it is intended to build an amplifying device which will probably be based initially on such a cylindrical sample as an amplifying substance.

A sketch of the cylindrical system in a rectangular waveguide is shown at Fig. 4. This problem can be generalized without much difficulty to the problem of two concentric

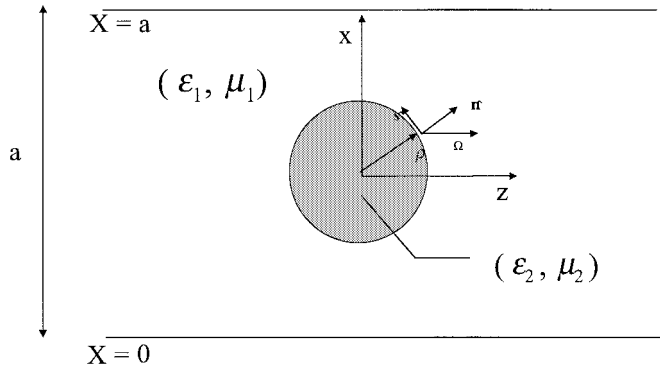


Fig. 4. Cross section of a rectangular waveguide with a cylindrical sample inside it. There is no  $Y$ -axis dependence.

cylinders where the inner cylinder represents the sample and the outer cylinder represents the quartz tube enclosure. This kind of dielectric structure is commonly used as a frequency filter and has been previously discussed in [28]–[30]. This case, however, is more general as both materials with both electric and magnetic material properties need be considered. For the sake of validation, two computationally different approaches have been used. Further validation of the results was made through measurements.

The first computational approach is based upon the equivalent currents formulation [31]. Beginning with the Maxwell's equations inside a waveguide [32]

$$\begin{aligned} \nabla \times \mathbf{E} &= -j\omega\mu \mathbf{H} - \mathbf{M} \\ \nabla \times \mathbf{H} &= j\omega\epsilon \mathbf{E} + \mathbf{J} \end{aligned} \quad (4)$$

where  $\mathbf{E}$  and  $\mathbf{H}$  are the electric and magnetic fields, respectively, and  $\mathbf{J}$  and  $\mathbf{M}$  are the electric- and magnetic-current density sources, respectively. We can obtain the wave equation inside the waveguide, assuming  $\partial/\partial y = 0$ , as in  $TE_{n0}$  modes, as follows:

$$\frac{\partial^2 E_y}{\partial x^2} + \frac{\partial^2 E_y}{\partial z^2} + w^2 \mu \epsilon E_y = j\omega\mu J_y + \frac{\partial M_x}{\partial z} - \frac{\partial M_z}{\partial x}. \quad (5)$$

A solution of this equation for a two-dimensional (2-D) cylinder scattering problem for a free-space boundary condition by the equivalent currents' formulation was employed in [31]. The application of a similar formulation to solve our problem is facilitated by replacing the free-space Green's function by the Green's function for a waveguide [32]. Unlike the purely dielectric case, complete Green's dyadic information is needed for both types of sources as follows.

- The Green's dyad element relating the electric field to electric sources (designated, respectively, by the superscript and subscript below)

$$\begin{aligned} G_{J_y}^{E_y}(x, z; x', z') \\ = \frac{-j}{a} \sum_{n=1}^{\infty} \frac{1}{k_{zn}} \sin\left(\frac{n\pi x}{a}\right) \sin\left(\frac{n\pi x'}{a}\right) e^{-jk_{zn}|z-z'|}. \end{aligned} \quad (6)$$

- The elements relating the magnetic field to electric sources

$$\begin{aligned}
 G_{J_y}^{H_x}(x, z; x', z') &= \pm \frac{1}{a} \sum_{n=1}^{\infty} \sin\left(\frac{n\pi x'}{a}\right) \sin\left(\frac{n\pi x}{a}\right) e^{-jk_{zn}|z-z'|} \\
 G_{J_y}^{H_z}(x, z; x', z') &= \frac{1}{a} \sum_{n=1}^{\infty} \frac{n\pi}{jk_{zn}a} \sin\left(\frac{n\pi x'}{a}\right) \cos\left(\frac{n\pi x}{a}\right) e^{-jk_{zn}|z-z'|}.
 \end{aligned} \tag{7}$$

- The elements relating the electric field to magnetic sources

$$\begin{aligned}
 G_{M_x}^{E_y}(x, z; x', z') &= \pm \frac{1}{a} \sum_{n=1}^{\infty} \sin\left(\frac{n\pi x'}{a}\right) \sin\left(\frac{n\pi x}{a}\right) e^{-jk_{zn}|z-z'|} \\
 G_{M_x}^{E_z}(x, z; x', z') &= \frac{j}{a} \sum_{n=1}^{\infty} \frac{n\pi}{k_{zn}a} \sin\left(\frac{n\pi x'}{a}\right) \cos\left(\frac{n\pi x}{a}\right) e^{-jk_{zn}|z-z'|}.
 \end{aligned} \tag{8}$$

- The elements relating the magnetic field to magnetic sources

$$\begin{aligned}
 G_{M_x}^{H_x}(x, z; x', z') &= -\frac{w\epsilon}{a} \sum_{n=1}^{\infty} \frac{1}{k_{zn}} \sin\left(\frac{n\pi x}{a}\right) \sin\left(\frac{n\pi x'}{a}\right) e^{-jk_{zn}|z-z'|} \\
 G_{M_x}^{H_z}(x, z; x', z') &= -\frac{w\epsilon}{a} \sum_{n=1}^{\infty} \frac{1}{k_{zn}} \cos\left(\frac{n\pi x}{a}\right) \cos\left(\frac{n\pi x'}{a}\right) e^{-jk_{zn}|z-z'|}.
 \end{aligned} \tag{9}$$

Using this Green's dyad, the employment of the equivalent current formulation is quite straightforward, resulting in the scattering matrix of the dielectric/magnetic post. A second formulation, using fictitious currents [29], was also employed. A comparison between the two methods and the published literature [30] for the case of a dielectric post is shown in Fig. 5. It can be seen that a good agreement exists between both the two computational methods and the previously published results. Although these results relate to dielectric samples, it is anticipated that similar accuracy would be achieved for magnetic posts as well. An experimental phase has been carried out as another validation of the calculation. The experiment included measuring the return loss by dielectric and magnetic samples within a rectangular waveguide using a vector network analyzer. These measurements also constitute part of the preparation for the microwave amplifying maser (see the fourth experiment below). The dimensions of the

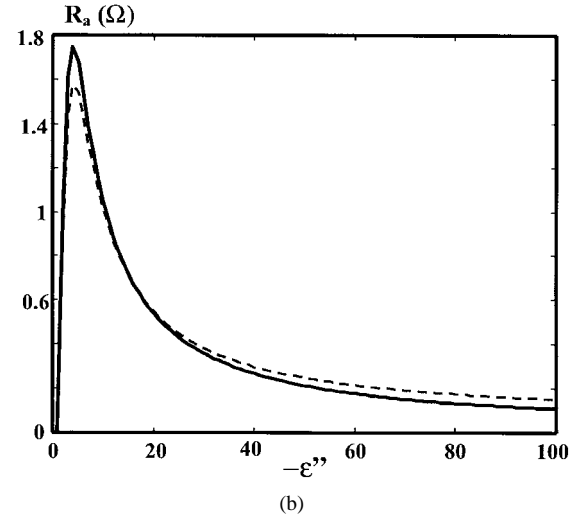
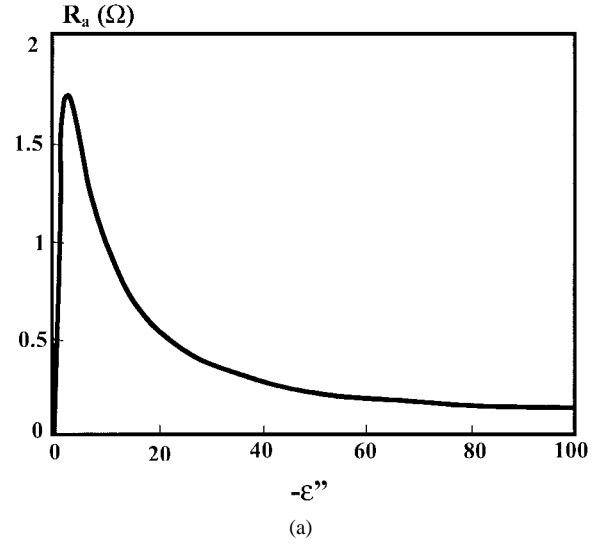


Fig. 5. Impedance matrix parameter  $Ra = \text{Real}(Z_{12})$  [see Fig. 8(b)]. As calculated for post with  $\epsilon' = 4$  and  $\epsilon''$  as the  $x$ -axis parameter, the post radius is  $r = 0.05a$  and the wavelength is  $\lambda = 1.4a$ . At (a) the results of [30], and at (b) the results of the fictitious currents (solid line) and equivalent currents (dashed line) calculation.

waveguide were  $a = 3.5$  cm and  $b = 1$  cm, and the operating frequency was 6.91 GHz. The dimensions of the waveguide were designed to fit within a given static magnet used for the spin microwave amplifying device, both in term of its geometry and magnetic field. The predicted and measured results obtained for an 8-mm-diameter Teflon cylinder placed at the center of the waveguide are shown in Fig. 6.

With the results of the above theoretical and experimental work, an application demonstration is to be carried out. This demonstration device is designed to directly evaluate the applicability of  $C_{60}$  in LC as an active maser amplifier device in terms of the aforementioned five aspects. We now present a theoretical treatment for the expected performance of such device as follows:

1) *Noise Temperature*: Noise temperature of optically pumped microwave masers was discussed in [14] with a typical energy level scheme of a three-level maser using an optically pumping solid-state maser, shown in Fig. 7(a). This

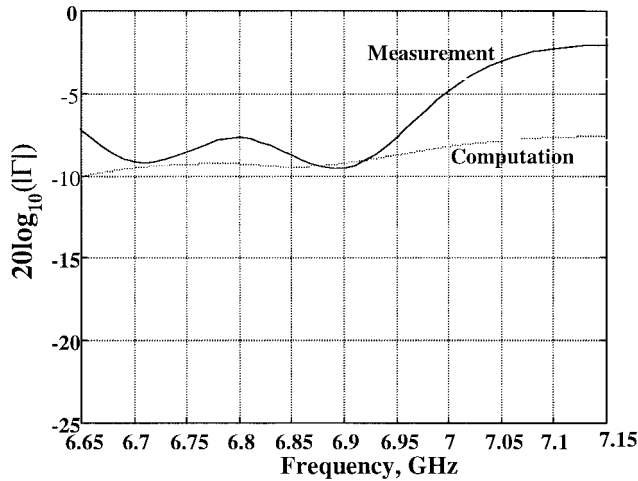


Fig. 6. Reflection coefficient of a Teflon post of radius of 8 mm, calculated and measured. The measurements were carried out with a nonstandard rectangular waveguide with dimensions  $a = 3.5$  cm,  $b = 1$  cm, designed to fit within the gap of the magnet. This causes difficulties in the design of a wide-band waveguide-to-coax adaptor, hence, the discrepancies between measurements and computation above 6.95 GHz.

energy level system has a noise temperature at equilibrium of [14]

$$|T_e| = T \left[ 1 + \frac{W_{21}}{w_{21}} \left[ \frac{w_{32}}{w_{21}} \cdot \frac{k_B T}{h\nu_{12}} \frac{W_{13}}{w_{31} + w_{32} + W_{13}} - 1 \right] \right]^{-1} \quad (10)$$

where  $T$  is the physical temperature in kelvin. In a typical case,  $W_{13} \gg w_{31} + w_{32}$  and  $W_{21} \ll w_{21}$ , we obtain

$$|T_e| \approx T \left[ \frac{w_{32}}{w_{21}} \cdot \frac{k_B T}{h\nu_{12}} - 1 \right]^{-1} \quad (11)$$

Due to the fact that solid-state optically pumped masers have  $w_{21}$ , which is highly temperature dependent [14], [15], there is a difficulty in operating these masers above cryogenic temperatures (as in ordinary microwave pumped solid-state masers). It can be seen from (11) that as  $w_{21}$  rises, so does the noise temperature. A schematic energy level diagram of the  $C_{60}$  in the LC case is shown at Fig. 7(b). At steady-state equilibrium, the expression for the noise temperature is

$$T_e \approx \frac{h\nu_{23}}{k_B \left[ \frac{w_d}{w_{32}} - \frac{h\nu_{23}}{k_B T} \right]} = T \left[ \frac{w_d}{w_{32}} \frac{k_B T}{h\nu_{32}} - 1 \right]^{-1} \quad (12)$$

At first sight, this expression seems similar to the one above, however, there are two important differences. Firstly,  $w_{32}$  is not strongly dependent upon the temperature (as in paramagnetic crystals) used at conventional EPR masers and remains at several microseconds even at room temperature (compared to nanoseconds and less in paramagnetic crystals at room temperature). Secondly, as shall be shown below, the possibility of a pulsed maser and not a CW maser is examined (due to pumping power restrictions). In a pulsed system, the pumped energy level is saturated with a strong laser pulse. For the  $C_{60}$  in the LC case, prior to the pulse excitation, the lower level of the spins [see Fig. 7(b), level 2]

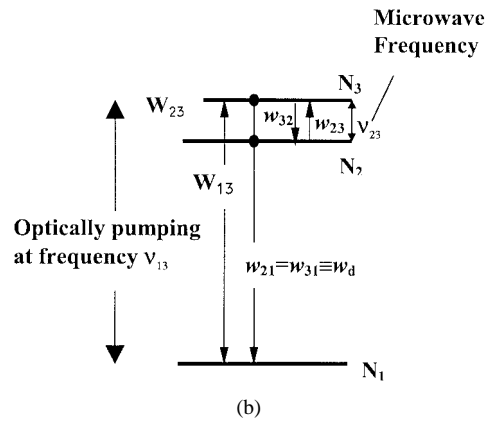
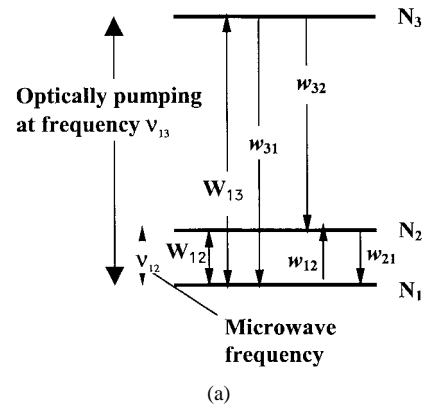


Fig. 7. Energy level scheme for “conventional” (a) optically pumped solid-state maser and (b) optically pumped  $C_{60}$  in LC. The  $w$ 's represents the transition rate, where  $W$  represents induced transitions.

is virtually empty. Also, the light excitation is spin selective, which gives a spin population difference of about  $50\times$  more than the ordinary Boltzmann population difference at 253 K (as we have seen in Section II). This means that the effective spin temperature immediately after the laser pulse is lower than 5 K and approaches zero as the selectivity of the process is improved, as in materials we intend to examine in the future. On the other hand, trying to obtain pulsed maser in the ordinary paramagnetic crystals case, even with complete selectivity in the process will not allow us, of course, to empty the lower level because at  $t = 0$ , the ground level of the maser frequency is fully populated.

Our discussion did not consider other noise factors in the system such as input line losses and cavity losses, which contribute to the noise temperature of the device. However, by careful construction, the contribution of these should not be substantial.

2) *Gain-Loss Balance*: One of the most important aspects related to maser action which have to be examined is the gain-loss balance of the maser material. In our experiments, a cylindrical sample was used. Let us examine the situation of cylindrical sample placed in the middle of a rectangular waveguide, as shown in Fig. 8(a). The equivalent transmission-line representation of this problem is shown in Fig. 8(b). The cylindrical sample impedance matrix calculation is based upon the above discussion (at the beginning of this section) and the inductive slit impedance matrix calculation is based on [28]

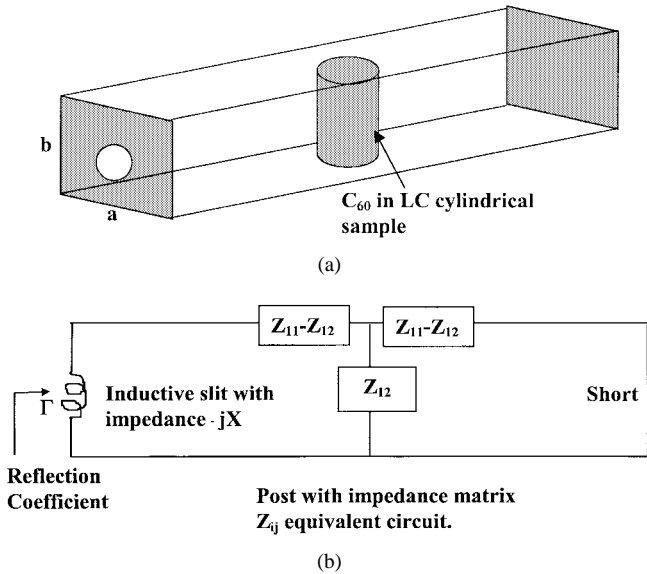


Fig. 8. (a) Maser cavity with the cylindrical sample inside it,  $a$  and  $b$  represent the waveguide dimensions. (b) The equivalent transmission-line representation of the cavity with the sample, which was used to calculate the reflection coefficient (see Fig. 6).

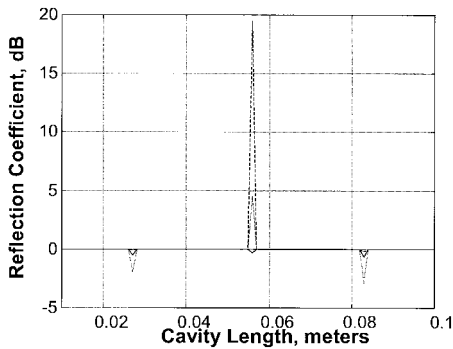


Fig. 9. Calculated reflection coefficient of maser cavity, shown in Fig. 8, in decibels as a function of sample properties and cavity length. The waveguide dimensions are  $a = 0.035$  m and  $b = 0.01$  m. RF frequency taken as 6.91 GHz. The inductive slit was taken with a diameter of 9 mm and the sample radius is 4 mm. Solid line: the reference case of sample properties  $\epsilon_r = 2 - 0.01j$  and  $\mu_r = 1 - 0j$ . Dotted line: the case of  $\epsilon_r = 2 - 0.01j$  and  $\mu_r = 1 + 0.001j$ . Dashed line: the case of  $\epsilon_r = 2 - 0.01j$  and  $\mu_r = 1 + 0.01j$ .

and [33]. Fig. 9 shows the resulting reflection coefficient of the structure presented in Fig. 8 for several sample types and cavity geometry. It can be seen that by placing the sample at the minimum of the electric field and at the maximum of the magnetic field, the dielectric losses are minimized and magnetic amplification is observed for typical dielectric and magnetic properties of  $C_{60}$  in LC.

3) *Pumping Power*: We are currently dealing with a phenomenon with a lifetime of the order of  $10 \mu s$  at room temperature. There is inherent uneconomical energy balance of pumping in optical frequencies and receiving microwave output. Also, the relatively short lifetime of the excited levels, before falling back to ground state cause the needed optical power for CW operation to be on the order of kilowatts for a sample of less than  $0.07 \text{ cm}^3$ . This implies that for CW operation, an intensive cooling must be added to the system,

along with very strong optical power. For that reason, we discuss the use of this material as a pulsed maser only. Other materials that are under investigation (see below) may enable CW operation much easier.

4) *Oscillation Buildup Time*: Use of the maser as a pulsed system requires that the oscillation buildup time must be much smaller than the lifetime of the phenomenon (the population inversion). The buildup time can be analyzed the same way as discussed in [34]. By taking the typical permeability and permittivity of Fig. 9 (dashed line), it is possible to calculate for a typical X-band cavity that the buildup time to reach a signal amplification of 30 dB is about 30 ns after the laser's excitation pulse (which, itself, lasts about 10 ns). This short buildup time enables the treatment of the maser as a steady-state phenomenon, as has been done above, and also enables the use of the system in pulsed mode.

5) *Maximum Gain, Bandwidth, and Saturation Power*: Since we are dealing with a typical number of  $10^{17}$  molecules of an active material with a population inversion  $\Delta N$  of about  $10^{16}$  molecules, saturation of this pulse system with a microwave pulse of maximum  $10 \mu s$  requires  $6 \times 10^{-8}$  J, or 6 mW. The bandwidth of the system is determined by the linewidth, shown in Fig. 1, typically about 27 MHz, although, it may be a bit smaller than that if one takes the gain influence into consideration [35]. Practical devices may increase the bandwidth by using several magnetic fields or use of a traveling-waves structure to increase the amount of amplifying material, causing the saturation power to increase accordingly [35].

It is concluded that a pulsed low-noise optically pumped maser is feasible with the above data and considerations. Other possibilities of novel electronic/EM devices which exploit these materials' properties are listed below.

a) *EM limiting devices*: These devices exploit the fact that the sample material is easily saturated by EM radiation. Using this property may protect sensitive receivers. Designing a proper microwave junction between the antenna and the receiver can do this. For small enough signals, the material sample dielectric and especially magnetic properties cause the signal to enter the receiver. However, for stronger EM signals, the sample loses its unique magnetic properties and the EM radiation is, by proper design of the microwave junction, diverted from the receiver and does not harm it. The small dielectric losses of the organic solvents used in these samples prevents the sample from heating up during this strong EM pulse.

b) *Phase shifter without losses*: The materials magnetic properties and positive  $\kappa''$  can be used with careful construction as a phase shifter, which prevents losses almost completely.

## IV. CONCLUSIONS

Based on the selective spin population due to light excitation, we have presented a new approach for a possible construction of a room-temperature optically pumped solid-state maser amplifying devices. We have demonstrated this possibility theoretically on  $C_{60}$  molecules dissolved in LC.

This device may be operated at room temperatures in pulse mode to amplify microwave pulses up to about 10- $\mu$ s long with a very low-noise temperature similar to the one obtained today via cryogenic cooling. The device may also sustain low-noise temperature at frequencies above 10 GHz, where today's cryogenic solid-state amplifiers becomes noisier. Other materials, such as  $C_{70}$  molecules dissolved in LC or Porphyrin  $H_2$  tetraphenyl porphyrin free base ( $H_2$ TPP), dissolved in either LC or toluene [7], [20], are currently under investigation and may prove an even better active materials (in terms of spin selectivity and excited state lifetime). Further applications of the investigated phenomenon have also been presented.

## REFERENCES

- [1] N. Bloembergen, "Proposal for a new type solid state maser," *Phys. Rev.*, vol. 104, p. 324, 1956.
- [2] H. E. D. Scovil, G. Feher, and H. Seidel, "Operation of a solid state maser," *Phys. Rev.*, vol. 105, p. 762, 1957.
- [3] A. McWhorter and J. Meyer, "Solid-state maser amplifier," *Phys. Rev.*, vol. 109, p. 312, 1958.
- [4] L. A. Sorin and M. V. Vlasove, *Electron Paramagnetic Resonance of Paramagnetic Crystals*. New York: Plenum Press, 1973.
- [5] R. DeGrasse, E. Schulz-DuBoise, and H. Scovil, "The three-level solid-state traveling-wave maser," *Bell Syst. Tech. J.*, vol. 38, p. 305, Mar. 1959.
- [6] R. Price *et al.*, "Radar echoes from Venus," *Science*, vol. 129, p. 751, 1959.
- [7] E. A. Ohm, "Project echo-receiving system," *Bell Syst. Tech. J.*, vol. 40, p. 1065, 1961.
- [8] R. L. Forward and H. P. Scott, "Application of a solid state ruby maser to an X-band radar system," in *IRE WESCON Conv. Rec.*, pt. 1, 1959, p. 119.
- [9] S. L. Bradford and C. Michel-Henri, *The Microwave Engineering Handbook*. London, U.K.: Chapman and Hall, 1993, vol. 3.
- [10] B. Thomas *et al.*, "The Parkes radio telescope modified for rapid receiver changes," *IEEE Antennas Propagat. Mag.*, vol. 39, no. 2, pp. 54-60, 1997.
- [11] G. W. Glass, D. L. Johnson, and G. G. Ortiz, "X-band ultra-low-noise maser amplifier performance," in *Temperature Electron. and High Temperature Superconduct.*, Stanley I. Raider, Ed., in *Proc. Electrochem. Soc. Symp.*, vol. 93-22, 1993, p. 333.
- [12] W. H. Carter, "The maser," *Science*, vol. 126, p. 810, 1957.
- [13] D. P. Devor, I. J. D'Haenens, and C. K. Asawa, "Microwave generation in Rubi due to population inversion produced by optical absorption," *Phys. Rev. Lett.*, vol. 8, p. 432, 1962.
- [14] H. Hsu and F. K. Tittle, "Optical pumping of microwave masers," *Proc. IEEE*, vol. 51, p. 185, Jan. 1963.
- [15] E. S. Sabisky and C. H. Anderson, "Solid-state optically pumped microwave masers," *IEEE J. Quantum Electron.*, vol. QE-3, pp. 287-295, July 1967.
- [16] A. Regev, D. Gamliel, V. Meiklyar, S. Michaeli, and H. Levanon, "Dynamics of  $^3C_{60}$  probed by electron paramagnetic resonance. Motional analysis in isotropic and liquid crystalline matrices," *J. Phys. Chem.*, vol. 97, p. 3671, 1993.
- [17] G. L. Closs, P. Z. Gautam, P. J. Krusic, S. A. Hill, and E. Wasserman, "Steady state and time resolved direct detection EPR spectra of fullerene triplets in liquid solution and glassy matrices. Evidence for dynamic John-Teller effect in triplets  $C_{60}$ ," *J. Phys. Chem.*, vol. 96, p. 5228, 1991.
- [18] H. Levanon, V. Meiklyar, A. Michaeli, S. Michaeli, and A. Regev, "Paramagnetic states and dynamics of photoexcited  $C_{60}$ ," *J. Phys. Chem.*, vol. 96, p. 6128, 1992.
- [19] J. A. Weil, J. R. Bolton, and J. E. Wertz, *Electron Paramagnetic Resonance*. New York: Wiley, 1994.
- [20] M. Terazima, N. Hirota, H. Shinohara, and Y. Saito, "Time-resolved EPR investigation of the triplet states of  $C_{60}$  and  $C_{70}$ ," *Chem. Phys. Lett.*, vol. 195-204, 1992.
- [21] H. Kiemle and H. Rothe, "The complex magnetic susceptibility of maser rubies at microwave frequencies," *Proc. IEEE*, vol. 52, p. 1243, Oct. 1964.
- [22] C. P. Poole Jr., "Electron spin resonance," in *A Comprehensive Treatise on Experimental Techniques*, 2nd ed. New York: Wiley, 1983.
- [23] M. Seehra, "New method for measuring the static magnetic susceptibility by paramagnetic resonance," *Rev. Sci. Instrum.*, vol. 39, no. 7, 1968.
- [24] O. Gonen and H. Levanon, "Time-resolved EPR spectroscopy of electron spin polarized ZnTPP triplets oriented in a liquid crystal," *J. Phys. Chem.*, vol. 89, p. 1637, 1985.
- [25] C. A. Stern, H. V. Willigen, and K. P. Dine, "Spin dynamics of  $C_{60}$  triplets," *J. Phys. Chem.*, vol. 98, p. 7464, 1994.
- [26] C. A. Stern, P. R. Levstein, H. V. Willigen, H. Linschitz, and L. Biczok, "FT-EPR study of triplet state  $C_{60}$  spin dynamics and electron transfer quenching," *Chem. Phys. Lett.*, vol. 204, no. 1-2, p. 23, 1994.
- [27] J. A. McMillian, *Electron Paramagnetism*. New York: Reinhold, 1968.
- [28] N. Marcuvitch, *Waveguide Handbook*. New York: Dover, 1965.
- [29] G. S. Sheaffer and Y. Leviatan, "Composite inductive posts in waveguide—A multifilament analysis," *IEEE Trans. Microwave Theory Tech.*, vol. 36, p. 779, Apr. 1988.
- [30] J. Abdunour and L. Marildon, "Scattering by dielectric obstacle in a rectangular waveguide," *IEEE Trans. Microwave Theory Tech.*, vol. 41, p. 1988, Dec. 1993.
- [31] K. Unshankar and A. Taflove, *Computational Electromagnetics*. Norwood, MA: Artech House, 1993.
- [32] J. Schwinger and C. Saxonm, *Discontinuities in Waveguides*. New York: Gordon and Breach, 1968.
- [33] R. E. Collin, *Field Theory of Guided Waves*. New York: IEEE Press, 1991.
- [34] A. E. Sigman, *Lasers*. Mill Valley, CA: Univ. Sci. Books, 1986.
- [35] H. N. Daghli *et al.*, *Low-Noise Microwave Amplifiers*. Cambridge, U.K.: Cambridge Univ. Press, 1968.



**Aharon Blank** received the B.S. degree in mathematics, physics, and chemistry (with honors) from the Hebrew University of Jerusalem, Jerusalem, Israel, in 1992, the M.S. degree in electrical engineering from Tel-Aviv University, Tel-Aviv, Israel, in 1997, and is currently working toward the Ph.D. degree from the Hebrew University of Jerusalem.

From 1989 to 1998, he served in the Israeli Air Force, first as a Cadet and then, from 1992, as an R&D Officer. His research interests are in the fields of EM propagation, radar cross section (RCS), radar-performance evaluation, magnetic resonance, and practical aspects photo-induced materials.



**Raphael Kastner** (S'80-M'82-SM'87) received the B.S. (*Summa cum laude*) and M.S. degrees from the Technion Israel Institute of Technology, Haifa, Israel, in 1973 and 1976, respectively, and the Ph.D. degree from the University of Illinois at Urbana-Champaign, in 1982.

From 1976 to 1988, he was with RAFAEL, Israel Armament Development Authority, where, from 1982 to 1986, he headed the antenna section. He was a Visiting Assistant Professor at Syracuse University from 1986 to 1987. Since 1988, he has been with the Department of Physical Electronics, Tel-Aviv University, Tel-Aviv, Israel, where he is currently an Associate Professor. His research interests include scattering analysis in the time and frequency domains, antennas, and antennas array.



**Haim Levanon** received the B.S., M.S., and Ph.D. degrees in chemistry from the Hebrew University of Jerusalem, Jerusalem, Israel, in 1963, 1965, and 1969, respectively.

He is currently a full Professor of chemistry at the Hebrew University of Jerusalem. His fields of research are time-domain electron paramagnetic resonance (EPR) spectroscopy, model photosynthesis, spin chemistry and physics, and LC's.